HIGH-RESOLUTION MEASUREMENTS OF MERCURY'S SURFACE COMPOSITION WITH THE MESSENGER X-RAY SPECTROMETER. Elizabeth A. Frank[1*], Larry R. Nittler[1], Audrey H. Vorburger[2], Shoshana Z. Weider[1], Richard D. Starr[3,4], and Sean C. Solomon[1,5], [1]Department of Terrestrial Magnetism, Carnegie Institution of Washington, Washington, DC 20015, USA. [2]Department of Earth and Planetary Sciences, American Museum of Natural History, New York, NY 10024, USA. [3]Physics Dept., The Catholic University of America, Washington, DC 20064, USA. [4]Solar System Exploration Division, NASA Goddard Space Flight Center, Greenbelt, MD 20771, USA. [5]Lamont-Doherty Earth Observatory, Columbia University, Palisades, NY 10964, USA. *E-mail: efrank@ciw.edu

Introduction: Since MESSENGER was inserted into orbit around Mercury in March 2011, the spacecraft's X-Ray Spectrometer (XRS) [1] has measured solar-induced X-ray fluorescence (XRF) from the top ~100 μm of the planet's surface and determined the abundances of key rock-forming elements, including Mg, Al, Si, S, Ca, Ti, and Fe [2–5]. Elements of low atomic number (Z), (i.e., Mg, Al, and Si) can be detected during periods of both quiet solar activity ("quiet Sun") and solar flares. The detection of higher-Z species, however, requires the heightened X-ray flux of flare periods. Analysis of the first orbital XRS measurements revealed a surface that is rich in Mg and S but depleted in Al, Ca, Ti, and Fe relative to typical terrestrial and lunar crustal materials [2]. Subsequent analyses with better spatial resolution have confirmed these results and indicate considerable heterogeneity in elemental abundances across the planet [3, 4], and we recently reported maps with global coverage of Mg/Si and Al/Si and partial maps of other major elements [5]. These maps, together with those of neutron absorption [6, 7], reveal the presence of several distinct geochemical terranes, although their boundaries do not always correspond to those identified from geological mapping or spectral reflectance. The terranes include a large ($>5\times10^6$ km^2) region containing the highest abundances of Mg, S, and Ca, as well as high neutron absorption (the high-Mg region or HMR), the interior volcanic smooth plains of the Caloris basin (CB), and portions of the northern volcanic plains (NVP) that have distinctive chemical compositions.

The spatial resolution of XRS measurements depends on the altitude and orientation of the spacecraft in its eccentric orbit. Since April 2014, MESSENGER has been orbiting at periapsis altitudes of <200 km and as low as ~20 km, compared with ≥200 km earlier in the mission. There is now an opportunity for XRS observations with substantially higher resolution (cross-track footprint size of as small as a few kilometers). Fortuitously, some of the lowest-altitude orbits coincided with periods of intense solar activity. This situation has yielded increased coverage and spatial resolution for XRS measurements of high-Z elements over Mercury's northern hemisphere. These improvements are notable because XRF of Fe requires the largest and least frequent solar flares, and until recently there have been few spatially resolved measurements of Fe on Mercury [4, 5]. Here we present updates to compositional maps of Mercury, including a substantial increase in Fe/Si coverage.

Data and Methods: The methods we use to analyze XRS data and generate maps have previously been reported [2–5]. Mg/Si and Al/Si maps incorporate both quiet-Sun and flare data and thus have almost complete global coverage. The other maps, however, are based solely on flare data and provide limited coverage in the northern hemisphere. Quiet-Sun data are spatially binned for the Mg/Si and Al/Si maps to improve statistical precision [5], but we use a smaller binning factor of 0.5° (versus the 3° used previously) to avoid substantially degrading the spatial resolution. We include data from April 2011 through November 2014, including flares that have not previously been analyzed. We have increased the areal coverage of Fe/Si measurements in the northern hemisphere by ~40% compared with the previous Fe/Si map [5].

Results and Discussion: Our new XRS maps (northward of 30°S) are shown in Figure 1. Also shown for comparison is the previously presented Mg/Si map [5], as well as maps of surface topography [8] and crustal thickness [9]. The improved resolution of our new full-mission Mg/Si and Al/Si maps is evident, and especially so in the Mg/Si map that we generated using only measurements with footprints <100 km across. These higher-resolution maps confirm the broad-scale geochemical features that have already been identified but also reveal smaller-scale chemical heterogeneities (e.g., within the HMR, CB, and NVP). Moreover, although not visible on the scale of Figure 1, the inner smooth plains of the Rachmaninoff basin (28°N, 60°E) have lower Mg/Si than the surrounding low-reflectance material. This difference had been unresolved until now.

We have also increased the coverage of higher-Z-element measurements in the northern hemisphere. In particular, with the new maps we confirm that the HMR has the highest S and Ca abundances on Mercury. From the analysis of several recent large flares we can also reveal—crucially—for the first time

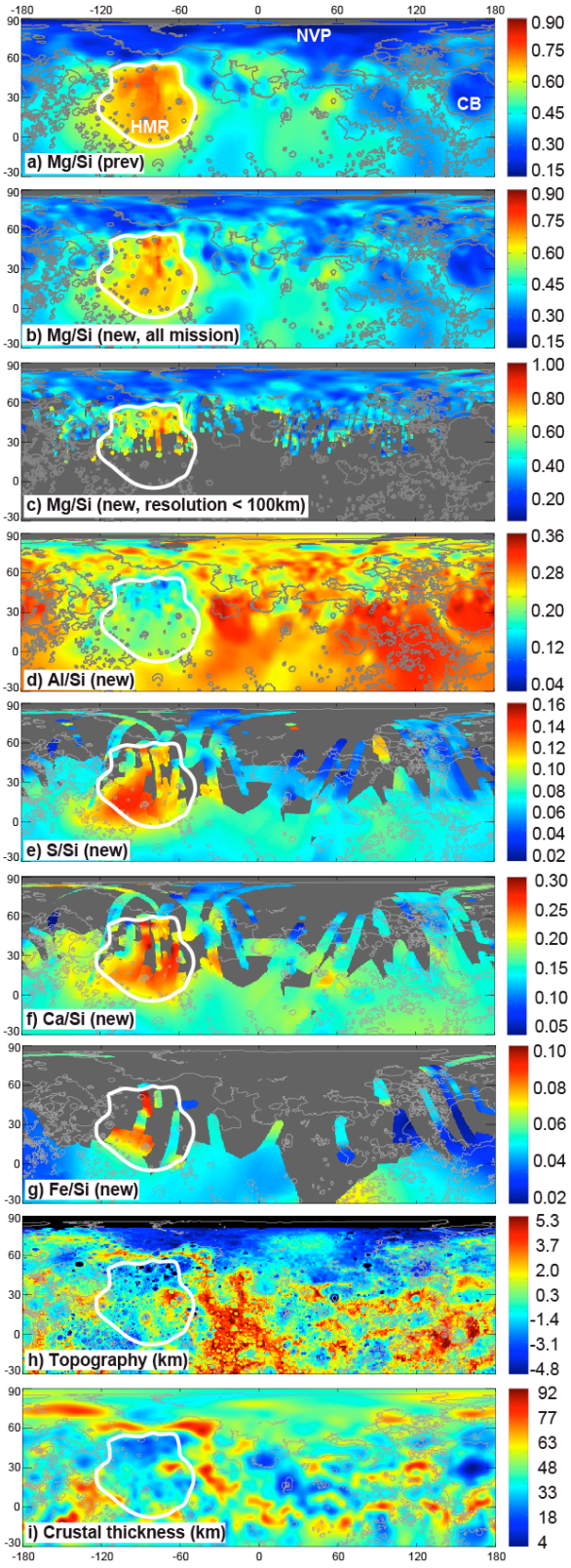

Figure 1. New compositional maps of Mercury (northward of 30°S in cylindrical projection) from XRS data. (a) Peviously published Mg/Si map, shown for comparison. (b) Map of all Mg/Si data to date. (c) Mg/Si generated only from measurements with footprints <100 km across. (d-g) Maps of measured elemental abundances normalized to Si. (h) Map of surface topography [8]. (i) Map of crustal thickness [9]. Light grey contours indicate outlines of smooth plains [10]. The HMR is outlined in white. The Caloris basin (CB) and northern volcanic plains (NVP) are marked in (a).

that the HMR exhibits the highest Fe/Si values (up to ~0.1, corresponding to >~2 wt% Fe) yet observed on the planet. The highest Fe/Si values are seen in portions of the HMR that also have the highest Mg/Si values and lowest topographic elevations. In the eastern portion of the HMR, where the topography is higher, we measure Fe/Si values that are lower and more similar to the planetary mean (~0.05). The relatively high Fe content of the HMR provides a plausible explanation for the high levels of thermal neutron absorption measured in this region [6, 7].

The HMR is also a region of thinner than average crust [9, 11], inferred from topography and free-air gravity anomaly measurements. The map of Mercury's crustal thickness, however, is derived with the assumption of a constant density contrast between crust and mantle. Our new constraints on the HMR composition may warrant a reevaluation of this assumption, given that the gravity measurements are sensitive to variations in crustal density as well as thickness. For example, the HMR is likely a product of high-degree partial melting and could even be a degraded ancient impact basin [5]. In such a case, the upper crust will be denser not only than the lower-Mg volcanic deposits of the other terranes but also than Mercury's bulk crust as a whole.

As MESSENGER's periapsis altitude continues to decline before the end of the mission in April 2015, we anticipate XRS observations with even better spatial resolution. Results from new and as-yet-unprocessed XRS data will be integrated with complementary datasets to generate increasingly detailed maps of Mercury's geologically and geochemically heterogeneous surface.

References: [1] Schlemm II C. E., et al. (2007) *Space Sci. Rev., 131,* 393-415. [2] Nittler L. R., et al. (2011) *Science, 333,* 1847-1850. [3] Weider S. Z., et al. (2012) *JGR, 117,* E00L05. [4] Weider S. Z., et al. (2014) *Icarus, 235,* 170-186. [5] Weider S. Z., et al. (2014) *EPSL,* submitted. [6] Peplowski P. N., et al. (2014) *Icarus,* submitted. [7] Lawrence D. J., et al. (2015) *LPS,* this volume. [8] Becker K. J., et al. (2014) *LPS, 45,* 2243. [9] James P. B., et al. (2015) *JGR Planets,* in press. [10] Denevi B. W., et al. (2013) *JGR Planets, 118,* 891-907. [11] Smith D. E., et al. (2012) *Science, 336,* 214-217.